pp. 1–15 (2019)

Lumped parameter heart model with valve dynamics

S. S. Simakov*

Abstract — In this work, the lumped parameter model of the left heart is presented. It is based on the concept of the time-varying elastance of myocardium and includes the model of the heart valve dynamics. Comparison of the models with instant and smooth valve opening and closing is given, as well as simulations of pathologies such as mitral valve stenosis and aortic valve insufficiency are addressed.

Keywords: Lumped model, cardiac dynamics, ventricle, auricle, aortic valve, mitral valve

MSC 2010: 65D25, 37M05, 92B99

The heart is the vitally important organ, which is responsible for the blood pumping through the whole organism. Its normal functioning is essential for the oxygen and nutrients delivery to tissues and for removing carbon dioxide and metabolic waste. The heart operates due to electrical stimulation initiated by the signals from the sinoatrial node generating the action potential. The latter passes through the heart and causes myocardium contraction by depolarization/repolarization of myocytes and actin-myosin interaction. The contraction of heart chambers pressurizes blood. Finally, the heart chambers eject blood to arteries and receive the new portion of blood from veins.

The detailed mathematical model of the heart function should account electrophysiology, soft tissue mechanics, and hydrodynamics. Some mathematical models simplify the subject. For instance, multi-scale integrated models of the cardiovascular system [3, 5, 15, 18–21, 24, 32] address functional behaviour of the heart in terms the of pressure–volume relationship PV, the cardiac output, the ejection fraction depending on the venous input (preload) conditions, arterial output (afterload) conditions, oxygen demand, etc. This concept is also applied to parts of the vascular network. These models operate with such variables as the volume of the heart chambers (auricles and ventricles), the pressure, and the blood flow. The conservation laws and semi-empirical hydrodynamic laws (e.g., Poiseuille law) relate these parameters together. The detailed spatial description is omitted and the models of this type are called lumped parameter or zero-dimensional (0D) models. The other common approach exploits electromechanical analogies between the variables and parameters of an electrical circuit (voltage, current, resistance, capacity, and inductance)

*Moscow Institute of Physics and Technology, Dolgoprudny 141701, Russia; Sechenov University, Moscow 119991, Russia. E-mail: simakov.ss@mipt.ru

The research was supported by the Russian Foundation for Basic Research 18-00-01524, 18-31-20048, 18-00-01661.

and mechanical variables and parameters (pressure, flow, hydraulic resistance due to blood viscosity, elasticity, inertia of blood). The resulting set of ordinary differential equations (ODEs) is very similar both for lumped hydrodynamic and electric circuit approaches. The number of equations depends on decomposition into compartments, which may include heart chambers, vascular regions, microcirculatory regions, aneurysms, etc. The extended reviews of basic principles and mathematical models both for the heart chambers and vascular regions can be found in [6, 25–27]. However, the electric circuit approach is difficult to apply to the detailed decomposition to many compartments due to the inexact consistency of electromechanic analogues [26].

In this work, we limit the discussion to the function of the left heart including left auricle, which receives blood from the pulmonary vein, and left ventricle, which ejects blood to the aorta. The fundamental concept of the heart function is time-varying elastance introduced for the first time in [28]. The lumped elastance of the heart chamber is defined as a slope of the PV diagram, i.e., the instant ratio $E = \Delta P/\Delta V$, where ΔV is the volume change due to the pressure change ΔP. The cardiac cycle is regarded as periodic change of the elastance E due to the electrical stimulation of the heart chamber by the action-potential [7, 28, 29]. During systole, the myocardium becomes much stiffer, so the tension rises to its maximum value and ejection performed. During diastole elastance falls to its minimum value, facilitating rapid filing of the chambers at low pressures (see [33] for details on dynamics of the cardiac cycle).

The other possible lumped descriptions of the heart function include force (muscle length relationship based on the Hill's three-element model of the muscle mechanical response [35]), pressure calculations based on the Laplace law and spherical shape assumption [8, 34] and more realistic cylindrical shape assumption [30] with cross-bridge kinetics and calcium regulation [31].

Essential elements of the heart are the valves between the auricles and ventricles and between ventricles and the aorta or the pulmonary artery. The valves help to maintain the unidirectional flow from venous to arterial parts, especially during the diastole phase when the heart chambers are filled with the new portion of venous blood. The times of valve opening and closing are rather small. The valve dynamics may cause a substantial effect on the cardiac output during these periods. The simplest description of the valve function is the instant opening/closing [15, 32]. The state of the valve may be set to change at predefined time moments within each heart period [15] or may be set according to the sign of the pressure drop across the valve [32]. An electrical analogue of the heart valve is a diode combined with a resistor. Valve motion is a complex process incorporating a pressure gradient across the valve, a vortex flow near the valve, a shear force acted on the valve leaflet [26]. The mechanical model accounting these features, is proposed in [16, 17]. It operates with the angle of the valve opening.

This paper is organized as follows. A model of the blood flow through the left heart is proposed in Subsection 1.1. It combines description of dynamics of the heart chambers (left auricle and ventricle) and the heart valves (mitral and aortic

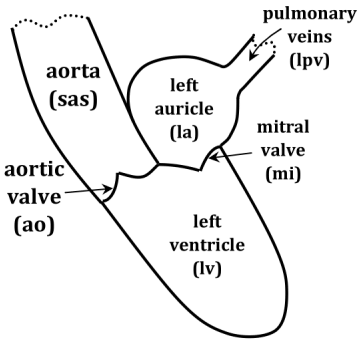

Figure 1. Scheme of the lumped model of the left heart.

valves). The appropriate numerical method and issues of the numerical implementation are discussed in Subsection 1.2. Comparison of heart dynamics simulated by models of instant and smooth valve opening and closing in Subsection 2.1. Simulations accounting valve pathologies, such as mitral valve stenosis and aortic valve insufficiency are considered in Subsection 2.2 and Subsection 2.3, respectively.

1. Materials and methods

The scheme of the left heart chambers and valves connections is shown in Fig. 1. We use the following notations for the indices: the diastolic phase d, the friction force fr, the maximum value max, the minimum value min, the pressure force p, the beginning of the P-wave pb, the duration of the P-wave pw, the resistance force r, the systole s, the peak of the systole $s1$, the end of the systole $s2$, whereas mi refers to the mitral valve, ao to the aortic valve, lpv to the input from left pulmonary veins to the left auricle, and sas to the entrance to the aorta (aortic sinus).

1.1. Lumped mathematical model of the heart and valve dynamics

Dynamics of the volume of a heart chamber with index k can be defined as

$$I_k \frac{\mathrm{d}^2 V_k}{\mathrm{d}t^2} + R_k \frac{\mathrm{d}V_k}{\mathrm{d}t} + E_k(t)\left(V_k - V_k^0\right) + P_k^0 = P_k, \quad k = lv, la \tag{1.1}$$

where V^0 is the reference volume of the chamber, P^0 is the reference pressure in the chamber, I is the inertia parameter, R is the hydraulic resistance of the compartment. Equation (1.1) is a modification of the model from [15]. Here we introduce time dependent elastance $E(t)$ and external pressure in the form $E(t)V^0 - P^0$. Using the concept of the variable elastance [28] we may set:

$$E(t) = E^d + \frac{E^s - E^d}{2} e(t), \quad 0 \leqslant e(t) \leqslant 1 \tag{1.2}$$

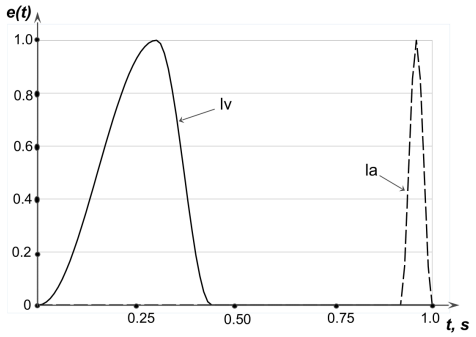

Figure 2. Activation functions of the left ventricle (lv) and left auricle (la).

which is similar to [16, 20]. The period of $e(t)$ equals to the duration of the heart cycle. For the left ventricle we set:

$$e_{lv}(t) = \begin{cases} 0.5\left(1-\cos\dfrac{t}{T_{s1}}\pi\right), & 0 \leqslant t \leqslant T_{s1} \\ 0.5\left(1+\cos\dfrac{t-T_{s1}}{T_{s2}-T_{s1}}\pi\right), & T_{s1} < t < T_{s2} \\ 0, & T_{s2} \leqslant t \leqslant T. \end{cases} \tag{1.3}$$

For the left auricle we set

$$e_{la}(t) = \begin{cases} 0, & 0 \leqslant t \leqslant T_{pb} \\ 0.5\left(1-\cos\dfrac{t-T_{pb}}{T_{pw}}2\pi\right), & T_{pb} < t < T. \end{cases} \tag{1.4}$$

The functions $e_{lv}(t)$ and $e_{la}(t)$ are shown in Fig. 2.

The flow rates through the chambers are described by the mass conservation conditions

$$\begin{aligned} \frac{\mathrm{d}V_{lv}}{\mathrm{d}t} &= Q_{mi} - Q_{ao} \\ \frac{\mathrm{d}V_{la}}{\mathrm{d}t} &= Q_{lpv} - Q_{mi}. \end{aligned} \tag{1.5}$$

The Poiseuille pressure drop conditions for the connections between the chambers and between the chamber and the appropriate vessel are

$$\begin{aligned} Q_{ao} &= g_{ao}(\vartheta_{ao})\frac{P_{lv}-P_{sas}}{R_{ao}} \\ Q_{mi} &= g_{mi}(\vartheta_{mi})\frac{P_{la}-P_{lv}}{R_{mi}} \\ Q_{lpv} &= \frac{P_{lpv}-P_{la}}{R_{lpv}} \end{aligned} \tag{1.6}$$

where $g(\vartheta) = \left\{ \vartheta^{\min} \leqslant \vartheta \leqslant \vartheta^{\max}, 0 \leqslant g(\vartheta) \leqslant 1 \right\}$ is a smooth monotonic valve function. For the closed valve it holds $g(\vartheta^{\min}) = 0$, for the fully opened valve $g(\vartheta^{\max}) = 1$.

The instant valve closing model uses the model with the prescribed valve function from [15]:

$$g(\vartheta) = \begin{cases} 0, & 0 \leqslant t < T_{\text{open}} \\ 1, & T_{\text{open}} \leqslant t \leqslant T_{\text{close}} \\ 0, & T_{\text{close}} < t \leqslant T \end{cases} \tag{1.7}$$

where $T^{ao}_{\text{open}} = 0.15\,\text{s}$, $T^{ao}_{\text{close}} = 0.33\,\text{s}$, $T^{mi}_{\text{open}} = 0.44\,\text{s}$, $T^{mi}_{\text{close}} = 1\,\text{s}$.

The model accounting valve dynamics uses the valve function:

$$\begin{aligned} g_{ao}(\vartheta_{ao}) &= \frac{(1-\cos\vartheta_{ao})^2}{(1-\cos\vartheta^{\max}_{ao})^2}, \qquad \vartheta^{\min}_{ao} \leqslant \vartheta_{ao} \leqslant \vartheta^{\max}_{ao} \\ g_{mi}(\vartheta_{mi}) &= \frac{(1-\cos\vartheta_{mi})^2}{(1-\cos\vartheta^{\max}_{mi})^2}, \qquad \vartheta^{\min}_{mi} \leqslant \vartheta_{mi} \leqslant \vartheta^{\max}_{mi} \\ g(\vartheta) &= \begin{cases} 0, & \vartheta < \vartheta^{\min} \\ 1, & \vartheta > \vartheta^{\max}. \end{cases} \end{aligned} \tag{1.8}$$

Our modification of the valve dynamics model [16, 17] states

$$\begin{aligned} \frac{\mathrm{d}^2\vartheta_{ao}}{\mathrm{d}t^2} &= -K^f_{ao}\frac{\mathrm{d}\vartheta_{ao}}{\mathrm{d}t} + (P_{lv}-P_{sas})\,K^p_{ao}\cos\vartheta_{ao} + K^b_{ao}Q_{ao}\cos\vartheta_{ao} - K^v_{ao}Q_{ao}\sin 2\vartheta_{ao}\tilde{f}_{ao} \\ \frac{\mathrm{d}^2\vartheta_{mi}}{\mathrm{d}t^2} &= -K^f_{mi}\frac{\mathrm{d}\vartheta_{mi}}{\mathrm{d}t} + (P_{la}-P_{lv})\,K^p_{mi}\cos\vartheta_{mi} + K^b_{mi}Q_{mi}\cos\vartheta_{mi} - K^v_{mi}Q_{mi}\sin 2\vartheta_{mi}\tilde{f}_{mi}. \end{aligned} \tag{1.9}$$

In (1.9) we introduce additional functions

$$\begin{aligned} \tilde{f}_{ao} &= \frac{1}{2}\left(1+\tanh\tilde{A}_{ao}\,(P_{lv}-P_{sas})\right), \qquad \tilde{A}_{ao} = 10 \\ \tilde{f}_{mi} &= \frac{1}{2}\left(1+\tanh\tilde{A}_{mi}\,(P_{la}-P_{lv})\right), \qquad \tilde{A}_{mi} = 10 \end{aligned} \tag{1.10}$$

which produce smooth switching in (1.9) according to the sign of the pressure drop across the appropriate valve.

Finally, the mathematical formulation of the cardiac dynamics model is the system of ordinary differential and algebraic equations (1.1)–(1.7) for the assumption of the instant valve opening and closing or the system (1.1)–(1.6) and (1.8)–(1.10) for the assumption of the smooth valve opening and closing. The beginning of the heart period is generally associated with the start of ventricle contraction (systole). This helps to define initial values for the initial value problems (1.1), (1.9):

$$\begin{aligned} V_k(0) &= V^0_k, \quad k = la, lv \\ \vartheta_l(0) &= 0, \quad l = ao, mi. \end{aligned}$$

Table 1. Coefficients of the model.

Parameter	Value	Parameter	Value
$E_{lv,s}$	2.0 mm Hg/ml	$\vartheta_{ao}^{\min}$	0°
$E_{lv,d}$	0.05 mm Hg/ml	$\vartheta_{ao}^{\max}$	75°
I_{lv}	10^{-5} mm Hg/ml	$\vartheta_{mi}^{\min}$	0°
R_{lv}	$4\cdot10^{-5}$ mm Hg·s/ml	$\vartheta_{mi}^{\max}$	75°
$E_{la,s}$	0.25 mm Hg/ml	P_{sas}	100 mm Hg
$E_{la,d}$	0.15 mm Hg/ml	P_{lpv}	37 mm Hg
I_{la}	10^{-5} mm Hg/ml	T_{s1}	0.3s
R_{la}	$4\cdot10^{-4}$ mm Hg·s/ml	T_{s2}	0.44s
T_{pw}	$0.08s$	T_{pb}	0.92s

The initial values are not significant, as we search periodic solutions of the above systems. The values of the coefficients are given in Table 1. Parameters of the valve dynamics model (1.9) were set according to [16].

1.2. Numerical implementation

If the model parameters are taken from the physiological range, the systems (1.1)–(1.7) and (1.1)–(1.6), (1.8)–(1.10) are stiff. It means that the solution has sudden variations during the valve opening and closing and gradual change during the other part of the heart cycle. Explicit numerical discretization of such ODEs may substantially limit the integration step due to the stability restrictions. The implicit one-step A– and L–stable method with the third-order approximation suits well for the numerical solution of the above problem. The method is constructed on the basis of predictor–corrector Obreshkov pairs [4].

Using the notations

$$\mathbf{y} = \left(V_{lv} \quad \frac{\mathrm{d}V_{lv}}{\mathrm{d}t} \quad V_{la} \quad \frac{\mathrm{d}V_{la}}{\mathrm{d}t} \quad \vartheta_{ao} \quad \frac{\mathrm{d}\vartheta_{ao}}{\mathrm{d}t} \quad \vartheta_{mi} \quad \frac{\mathrm{d}\vartheta_{mi}}{\mathrm{d}t} \right)^T \tag{1.11}$$

$$g_5(y_5) = g_{ao}(\vartheta_{ao}), \quad g_7(y_7) = g_{mi}(\vartheta_{mi}), \quad \tilde{R}_{lpv} = \frac{1}{R_{lpv}} \tag{1.12}$$

and eliminating $P_{lv}, P_{la}, Q_{ao}, Q_{mi}, Q_{lpv}$ from (1.1), (1.5), (1.6), (1.8), one may obtain the following system of the first order nonlinear ODEs

$$\frac{\mathrm{d}\mathbf{y}}{\mathrm{d}t} = \mathbf{f}(t, \mathbf{y}) \tag{1.13}$$

where

$$\begin{aligned} f_1 =& y_1 \\ f_2 =& \frac{1}{I_{lv}} \left(\left(\frac{\tilde{R}_{lpv} + g_7}{G} - R_{lv} \right) y_2 + \frac{g_7}{G} y_4 - e_{lv}(t) \left(y_1 - V_{lv}^0 \right) + P_{lv}^0 \right. \\ & \left. + \frac{g_5 \left(\tilde{R}_{lpv} + g7 \right)}{G} P_{sas} - \frac{g_7}{G} P_{lpv} \right) \end{aligned}$$

$$
\begin{aligned}
f_3 =& y_4 \\
f_4 =& \frac{1}{I_{la}}\left(\frac{g_7}{G}y_2+\left(\frac{g_5+g_7}{G}-R_{la}\right)y_4-e_{la}(t)\left(y_3-V_{la}^0\right)+P_{la}^0\right. \\
&\left.+\frac{g_5g_7}{G}P_{sas}-\frac{g_5+g_7}{G}\tilde{R}_{lpv}P_{lpv}\right) \\
f_5 =& y_6 \\
f_6 =& \frac{1}{G}\left(\left(\tilde{R}_{lpv}+g_7\right)y_2+g_7y_4+\left(g_5\left(\tilde{R}_{lpv}+g_7\right)-G\right)P_{sas}-g_7\tilde{R}_{lpv}P_{lpv}\right) \\
&\times\left(K_{ao}^p\cos y_5+g_5\left(K_{ao}^b\cos y_5-K_{ao}^v\sin 2y_5\tilde{f}_{ao}\right)\right) \\
f_7 =& y_8 \\
f_8 =& \frac{1}{G}\left(\tilde{R}_{lpv}y_2+g_5y_4+g_5\tilde{R}_{lpv}P_{sas}-g_5\tilde{R}_{lpv}P_{lpv}\right) \\
&\times\left(K_{mi}^p\cos y_7+g_7\left(K_{mi}^b\cos y_7-K_{mi}^v\sin 2y_7\tilde{f}_{mi}\right)\right)
\end{aligned}
\tag{1.14}
$$

$$
G=-\tilde{R}_{lpv}(g_5+g_7)-g_5g_7 \tag{1.15}
$$

$$
\begin{aligned}
\tilde{f}_{ao} =& \frac{1}{2}\left(1+\tanh\frac{\tilde{A}_{ao}}{G}\left[\left(\tilde{R}_{lpv}+g_7\right)y_2+g_7y_4+\left(g_5\left(\tilde{R}_{lpv}+g_7\right)-G\right)P_{sas}-g_7\tilde{R}_{lpv}P_{lpv}\right]\right) \\
\tilde{f}_{mi} =& \frac{1}{2}\left(1+\tanh\frac{\tilde{A}_{mi}}{G}\left[-\tilde{R}_{lpv}y_2+g_5y_4-g_5\tilde{R}_{lpv}\left(P_{sas}+P_{lpv}\right)\right]\right).
\end{aligned}
\tag{1.16}
$$

According to the Obreshkov pairs integration method [4, 14] we consider the extended system of (1.13)

$$
\frac{\mathrm{d}\mathbf{y}}{\mathrm{d}t}=\mathbf{f}(t,\mathbf{y}),\qquad \frac{\mathrm{d}\mathbf{w}}{\mathrm{d}t}=\frac{\partial\mathbf{f}}{\partial t}+\frac{\partial\mathbf{f}}{\partial\mathbf{y}}\mathbf{f} \tag{1.17}
$$

where $\mathbf{w}=\mathrm{d}\mathbf{y}/\mathrm{d}t$. General single-step implicit Runge–Kutta method for the numerical discretization of (1.17) can be stated as

$$
\mathbf{R}\left(\mathbf{y}^{n+1}\right)=\sum_{k=0}^{1}\left[a_k\mathbf{y}-\tau b_k\mathbf{f}-\tau^2c_k\left(\frac{\partial\mathbf{f}}{\partial t}+\frac{\partial\mathbf{f}}{\partial\mathbf{y}}\mathbf{f}\right)\right]_{t=t_{n+k},\mathbf{y}=\mathbf{y}^{n+k}} \tag{1.18}
$$

which is solved by the Newton's method as

$$\mathbf{y}_{s+1}^{n+1} = \mathbf{y}_s^{n+1} - \mathbf{B}^{-1}\left(t^{n+1}, \mathbf{y}^{n+1}\right)\mathbf{R}\left(\mathbf{y}_s^{n+1}\right), \quad s = 1,2,\ldots, \quad \mathbf{y}_0^{n+1} = \mathbf{y}^n \tag{1.19}$$

where

$$\begin{gathered}\mathbf{B} = \frac{\partial \mathbf{R}}{\partial \mathbf{y}^{n+1}} = \mathbf{E} - \tau b \frac{\partial \mathbf{f}}{\partial \mathbf{y}} - \tau^2 c \left(\frac{\partial}{\partial \mathbf{y}} \left(\frac{\partial \mathbf{f}}{\partial t} \right) + \left(\frac{\partial \mathbf{f}}{\partial \mathbf{y}} \right)^2 + \mathbf{C} \right) \\ \mathbf{C} = \left\{ \left(\frac{\partial}{\partial y_j} \left(\frac{\partial \mathbf{f}}{\partial \mathbf{y}} \right) \right) \mathbf{f} \right\}.\end{gathered} \tag{1.20}$$

According to [14] the parameters

$$\begin{gathered}a_1 = 1, \quad a_0 = -1, \quad b_0 = \frac{1}{2} + c_0 + c_1, \quad b_1 = \frac{1}{2} - c_0 - c_1 \\ c_1 = c_0 - \frac{1}{6}, \quad c_1 = 0\end{gathered} \tag{1.21}$$

define the numerical scheme of the third order approximation, which is both A- and L-stable. This scheme is used in this work for the numerical simulations.

2. Results

In this section, we consider three groups of simulations. The first group is comparison of the model with instant valve opening and closing and the model with the smooth valve function. The second and third groups address simulations of pathological cases. We consider the impact of a stenosis of the mitral valve and an aortic insufficiency on the cardiac output.

2.1. Comparison of valve closing models

The outputs of the model with the smooth valve function (1.1)–(1.6), (1.8)–(1.10) are referred to as model A. The outputs of the model with the instant valve opening and closing (1.1)–(1.7) are referred to as model B. The results of the simulations are shown in Figs. 3, 4, and 5. In all simulations, periodic solutions are observed starting from the third cardiac cycle. The times of the valve opening and closing in the model A with the valve dynamics is 0.05 s, but it is sufficient for the substantial differences in the cardiac outputs for models A and B.

The pressures, flow rates and volumes for model A shown in Figs. 3, 4, and 5 are in a good agreement with physiological data from [1, 23]. The systolic pressure in the left ventricle equals to the well-known value of 120 mm Hg. The systolic flow rate through the aortic valve equals to 900 ml/s, which corresponds to data for the aorta with diameter 3 cm. The systolic flow rate through the mitral valve is 300 ml/s. The volume of the left ventricle changes in the range from 50 to 120 ml. The volume of the left auricle changes in the range from 40 to 60 ml. Model A will

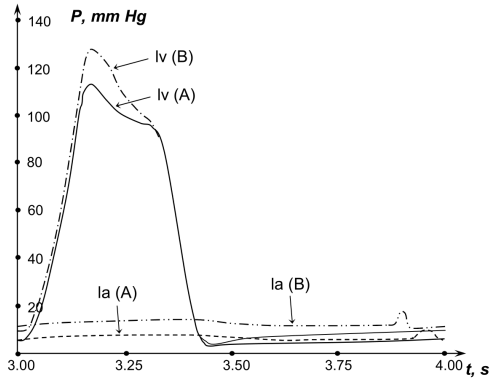

Figure 3. Pressure in the left ventricle and auricle (A — valve dynamics, B — instant valve opening/closing).

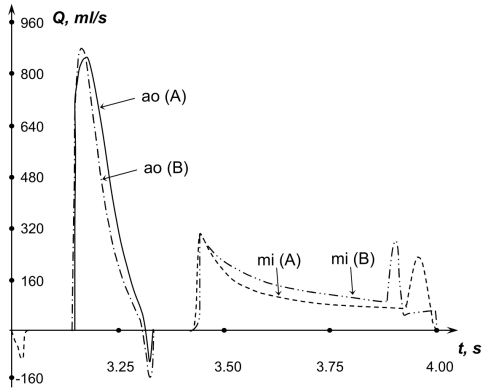

Figure 4. Flow rate through the aortic and mitral valves (A — valve dynamics, B — instant valve opening/closing).

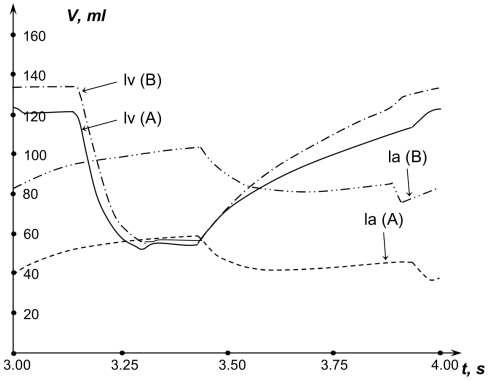

Figure 5. Volume of the left ventricle and auricle (A — valve dynamics, B — instant valve opening/closing).

also be used as the reference model with the normal conditions in the comparisons in Subsections 2.2 and 2.3.

The most pronounced difference between models A and B is the change of the systolic pressure in the left ventricle ($P^A_{lv,syst} = 120$ mm Hg, $P^B_{lv,syst} = 130$ mm Hg, see Fig. 3). The systolic value of the flow through the aortic valve is achieved 0.05 s later in model A than in model B. It causes substantial changes in the dynamics of the volumes of the chambers (see Fig. 5).

According to physiological data [1, 23] one of the well-known effects of the valve closing is the small backward flow from the aorta to the left ventricle at the end of the systole (aortic regurgitation). It results from the sudden decrease of the pressure in the ventricle, which occurs earlier than the full aortic valve closing completes. This effect is observed as a negative flow in both models A and B (see Fig. 4). Unfortunately, the backward flow in model B has no physiological sense because the instantly closed valve should immediately terminate the back flow. The negative flow in model B may be explained either by the numerical instability due to the discontinuous change of the valve function (1.7) or by inappropriate setting of the predefined intervals of the valve opening and closing in (1.7). Model A conforms to physiological data and produces realistic dynamics of the basic parameters of the cardiac cycle. Model B may be adjusted to the measured patient data, but it requires manual fitting in every case. It makes model B less useful for patient-specific applications.

2.2. Mitral valve stenosis

Mitral valve stenosis is a pathology caused by narrowing of the atrioventricular lumen between the left auricle and the left ventricle due to the coalescence of the mitral valve leaflets. The result of the mitral valve stenosis is the decrease of the flow from the auricle to the ventricle and associated reduction of the stroke volume and the cardiac output. Following [16], we model mitral valve stenosis by 30% decrease of the maximum opening angle $\vartheta^{\max}_{mi}$, which decreases the lumen by 25%. The results of the simulations are shown in Figs. 6 and 7.

First, we observe that the change of the opening of the mitral valve impact dynamics of the aortic valve. The moment of aortic valve opening is delayed by 0.05 s compared to the normal conditions. The observed changes of the systolic pressure in the left auricle from 115 to 110 mm Hg and in the left ventricle from 8 to 10 mm Hg are not significant. The pronounced effect is observed for the flow rate and the volume of the heart chambers. Figure 6 shows the decrease of the systolic blood flow through the aortic valve from 900 to 560 ml/s. The peak of the systole is delayed by 0.05 s compared to the reference conditions. This conforms with the delayed aortic valve opening. The shape of the mitral flow curve changes significantly. The first maximum at the beginning of the diastole and the negative flow at the end of the cardiac cycle disappear (see Fig. 6). Substantial decrease of the maximum of left ventricle volume from 120 to 85 ml is observed in Fig. 7. The volume of the left auricle increases from 40 to 50 ml.

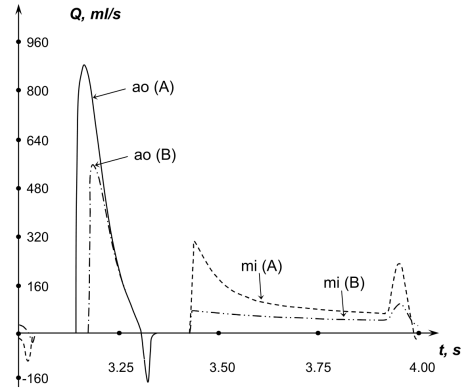

Figure 6. Flow rate through the aortic and mitral valves (A — normal conditions, B — mitral valve stenosis).

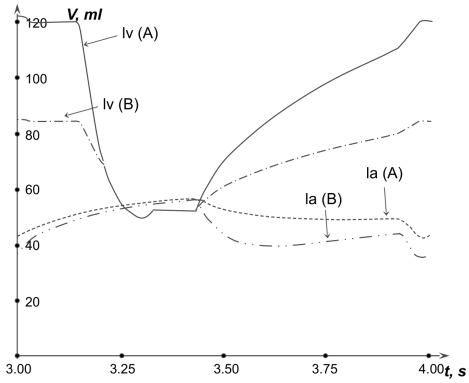

Figure 7. Volume of the left ventricle and auricle (A — normal conditions, B — mitral valve stenosis).

Thus, the model reproduces the known facts that the mitral valve stenosis increases the load to the left auricle, which may develop its hypertrophy. The mitral valve stenosis causes a substantial decrease in the cardiac output, which can be evaluated on the basis of patient-specific simulations.

2.3. Aortic insufficiency

Aortic insufficiency (aortic regurgitation) is the incompetence of the aortic valve that causes increased backward flow from the aorta into the left ventricle during the diastole. The reasons for aortic insufficiency include aortic root dilation, valvular degeneration, intrinsic features, etc. Aortic valve insufficiency is modelled similar to [16] by the increase of the minimum opening angle $\vartheta_{ao}^{\min}$ from 0° to 25°. The results of the simulations are shown in Figs. 8 and 9.

First, we observe that the change of the aortic valve dynamics affects mitral valve dynamics. The moment of mitral valve opening keeps ahead by 0.05 s compared to the normal conditions. The pressure in the left auricle remains the same.

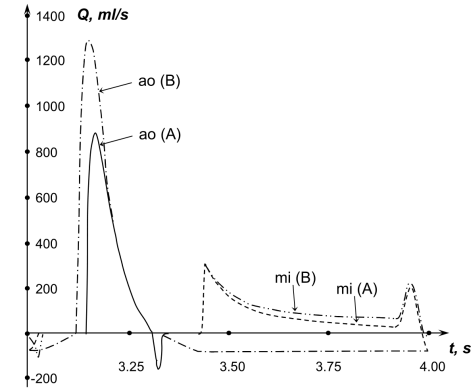

Figure 8. Flow rate through the aortic and mitral valve (A — normal conditions, B — aortic regurgitation).

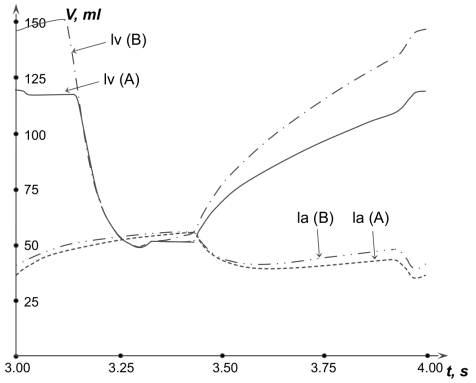

Figure 9. Volume of the left ventricle and auricle(A — normal conditions, B — aortic regurgitation).

The change of the peak pressure in the left auricle from 115 to 125 mm Hg and in the left ventricle from 8 to 10 mm Hg is not significant.

The substantial increase of the systolic blood flow rate through the aortic valve from 900 to 1300 ml/s is shown in Fig. 8. The systolic peak keeps ahead by 0.05 s relative to the reference conditions. It corresponds to the early aortic valve opening. One may note that the increase of the systolic flow is compensated by the reverse flow during diastole, but such conditions cause the substantial overload of the left ventricle and aorta resulting in their hypertrophy. The apparent effect of the aortic insufficiency is the negative flow of 70 ml/s during diastole, shown in Fig. 8. Substantial increase of the maximum of left ventricle volume from 120 to 150 ml is shown in Fig. 9, which also means possible development of its hypertrophy.

3. Discussion

The proposed lumped models of cardiac dynamics are based on the physical principles and provide performing physiologically correct simulations of the healthy

heart and the heart with certain diseases. The advantage of such approach is its low computational cost and a small number of parameters which can be identified in a conventional clinic.

The heart valve function $g(\vartheta)$ produces significant impact on cardiac dynamics. The instant valve opening and closing model (1.7) simplifies the mathematical formulation. In principle, the time moments of the valve opening and closing can be determined for the patient from echocardiography. However, the assumption of the instant opening and closing does not correspond to the physiological observation. The assumption also produces numerical instability in simulations. The model with heart valve dynamics provides better agreement with the physiological data. The coupling of the lumped heart model with the 1D haemodynamic model [2] produces a closed model of the cardiovascular network.

The drawbacks of the proposed lumped heart models are the lack of spatial details and the absence of the heart rate adaptation. The heart rate variability is an essential phenomenon for some clinical applications such as simulations of coronary circulation during cardiac pacing and tachycardia [9] and virtual assessment of the fractional flow reserve [10, 11].

Patient-specific identification of the model parameters including heart rate, angles of valve opening, the volume of chambers can be performed in a regular clinic through echocardiography and other conventional methods. The measurement of other model parameters (inertia coefficient, hydraulic resistance, variable elastance function) can be done only in the scope of a specific clinical research. In medical applications, these parameters should be determined by fitting known measured and computed variables (e.g., chamber volume dynamics, cardiac output, etc.).

References

1. K. Barret, H. Brooks, S. Boitano, and S. Barman, *Ganong's Review of Medical Physiology*. 23rd edition, The McGraw-Hill, 2010.

2. N. Bessonov, A. Sequeira, S. Simakov, Yu. Vassilevski, and V. Volpert, Methods of blood flow modelling. *Math. Modelling Natur. Phenomena* **11** (2016), No. 1, 1–25.

3. A. G. Borzov, S. I. Mukhin, and N. V. Sosnin, Conservative schemes of matter transport in a system of vessels closed by the heart, *Diff. Equ.* **48** (2012), No. 7, 919–928.

4. J. C. Butcher and P. Sehnalová, Predictorcorrector Obreshkov pairs. *Computing* **95** (2013), No. 5, 355–371.

5. D. Canuto, K. Chong, C. Bowles, E. P. Dutson, J. D. Eldredge, and P. Benharash, A regulated multiscale closed-loop cardiovascular model, with applications to hemorrhage and hypertension. *Int. J. Numer. Methods Biomed. Engrg.* (2018), e2975.

6. M. Capoccia, Development and characterization of the arterial Windkessel and its role during left ventricular assist device. *Artificial Organs* **39** (2015), No. 8, E138–E153.

7. K. B. Campbell, A. M. Simpson, S. G. Campbell, H. L. Granzier, and B. K. Slinker, Dynamic left ventricular elastance: a model for integrating cardiac muscle contraction into ventricular pressure-volume relationship, *J. Appl. Physiology* **104** (2008), No. 4, 958–975.

8. V. Diaz-Zuccarini and J. LeFevre, An energetically coherent lumped parameter model of the left

ventricle specially developed for educational purposes, *Computers in Biology and Medicine* **37**, (2007), 774–784.

9. T. M. Gamilov, F. Liang, and S. S. Simakov, Mathematical modeling of the coronary circulation during cardiac pacing and tachycardia. *Lobachevskii J. Math.* **40** (2019), No. 4, 448–458.
10. D. G. Gognieva, A. L. Syrkin, Yu. V. Vassilevski, et.al., Noninvasive assessment of fractional flow reserve using mathematical modeling of coronary flow. *Kardiologiya* **58** (2018), No. 12, 85–92 (in Russian).
11. D. G. Gognieva, T. M. Gamilov, R. A. Pryamonosov, et.al., Noninvasive assessment of the fractional reserve of coronary blood flow with a one-dimensional mathematical model. Preliminary results of the pilot study. *Russ. J. Cardiology* **24** (2019), No. 3, 60–68.
12. F. Kappel and R. O. Peer, A mathematical model for fundamental regulation processes in the cardiovascular system, *J. Math. Biology* **31** (1993), 611–631.
13. Y. S. Kim, E.-H. Kim, H.-G. Kim, E. B. Shim, K.-S. Song, and K. M. Lim, Mathematical analysis of the effects of valvular regurgitation on the pumping efficacy of continuous and pulsatile left ventricular assist devices, *Integrative Medicine Research* **5** (2016), 22–29.
14. A. S. Kholodov, A. I. Lobanov, and A. V. Evdokimov, Numerical schemes for solving stiff ordinary differential equations in the space of undetermined coefficients. MFTI, Moscow, (1985), p.49 (in Russian).
15. A. S. Kholodov, Some dynamical models of multi-dimensional problems of respiratory and circulatory systems including their interaction and matter transport. *Computer Models and Medicine Progress*. Nauka, Moskva, 2001, 127–163 (in Russian).
16. Th. Korakianitis and Y. Shi, Numerical simulation of cardiovascular dynamics with healthy and diseased heart valves. *J. Biomechanics* **39** (2006), No. 11, 1964–1982.
17. Th. Korakianitis and Y. Shi, A concentrated parameter model for the human cardiovascular system including heart valve dynamics and atrioventricular interaction. *Medical Engrg.&Physics* **28** (2006), 613–628.
18. F. Liang and H. Liu, A closed-loop lumped parameter computational model for human cardiovascular system *JSME Int. J. Series C* **48** (2005), No. 4, 484–493.
19. F. Liang and H. Liu, Simulation of hemodynamic responses to the valsalva maneuver: an integrative computational model of the cardiovascular system and the autonomic nervous system, *J. Physiological Sci.* **56** (2006), No. 1, 45–65.
20. F. Liang, S. Takagi, R. Himeno, and H. Liu, Multi-scale modeling of the human cardiovascular system with applications to aortic valvular and arterial stenosis, *Medical & Biological Engineering & Computing* **47** (2009), 743–755.
21. F.Y. Liang, S. Takagi, R. Himeno, and H. Liu, Biomechanical characterisation of ventriculararterial coupling during aging: A multi-scale model study, *J. Biomechanics* **42** (2009), No. 6, 692–704.
22. M. S. Olufsen, J. T. Ottesen, H. T. Tran, L. M. Ellwein, L. A. Lipsitz, and V. Novak, Blood pressure and blood flow variation during postural change from sitting to standing: model development and validation, *J. Appl. Physiology* **99** (2005), No. 4, 1523–1537.
23. R. F. Schmidt and G. Thews, *Human Physiology*. Vol. 2, 2nd edition. Springer-Verlag, Berlin–Heidelberg, 1989.
24. S. S. Simakov and A. S. Kholodov, Computational study of oxygen concentration in human blood under low frequency disturbances. *Math. Models Comp. Simul.* **1** (2009), No. 2, 283–295.
25. S. S. Simakov, Modern methods of mathematical modeling of blood flow using reduced order methods. *Comp. Research Modeling* **10** (2018), No. 5, 581–604 (in Russian).

26. Y. Shi, P. Lawford, and R. Hose, Review of Zero-D and 1-D Models of Blood Flow in the Cardiovascular System, *Biomed. Engrg. OnLine* **10** (2011), 33.

27. E. B. Shim, J. Y. Sah, and C. H. Youn, Mathematical modelling of cardiovascular system dynamics using a lumped parameter method. *Japan. J. Physiology* **54** (2004), 545–553.

28. H. Suga, Theoretical analysis of a left-ventricular pumping model based on the systolic time-varying pressure-volume relatio. *IEEE Transactions on Biomedical Engineering* **18** (1971), No. 1, 47–55.

29. H. Suga, Cardiac energetics: from E_{MAX} to pressure-volume area. *Clinical Experim. Pharmacol. Physiol.* **30** (2003), 580–585.

30. F. A. Syomin, M. V. Zberia, N. A. Koubassov, and A. K. Tsaturyan, Mathematical modelling of the dependence of the performance of the left ventrical of the heart on preload and afterload. *Biophysics* **60** (2015), No. 6, 983-987.

31. F. A. Syomin and A. K. Tsaturyan, A simple model of cardiac muscle for multiscale simulation: Passivemechanics, crossbridge kinetics and calcium regulation, *J. Theoretical Biology* **420** (2017), No. 7, 105–116.

32. P. R. Trenhago, L. G. Fernandes, L. O. Müller, P. J. Blanco, and R. A. Feijóo, An integrated mathematical model of the cardiovascular and respiratory systems. *Int. J. Numer. Methods Biomed. Engrg.* (2016), e02736.

33. K. R. Walley, Left ventricular function: time-varying elastance and left ventricular aortic coupling. *Critical Care* **20** (2016), No. 270.

34. J. Werner, D. Bohringer, and M. Hexamer, Simulation and prediction of cardiotherapeutical phenomena from a pulsatile model coupled to the Guyton circulation model, *IEEE Trans. Biomed. Engrg.* **49**, (2002), 430–439.

35. M. Zacek and E. Krause, Numerical simulation of the blood flow in the human cardiovascular system. *J. Biomechanics* **29** (1996), 13–20.